

Synthesis and Mössbauer Spectroscopy of Formal Tin(II) Dichloride and Dihydride Species Supported by Lewis Acids and Bases

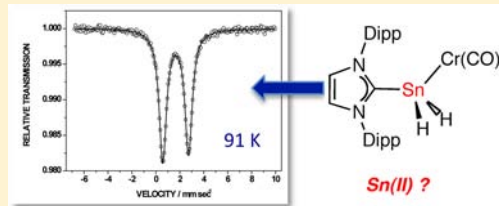
S. M. Ibrahim Al-Rafia,[†] Olena Shynkaruk,[†] Sean M. McDonald,[†] Sean K. Liew,[†] Michael J. Ferguson,[†] Robert McDonald,[†] Rolfe H. Herber,^{*,‡} and Eric Rivard^{*,†}

[†]Department of Chemistry, University of Alberta, 11227 Saskatchewan Dr., Edmonton, Alberta, Canada T6G 2G2

[‡]Racah Institute of Physics, Hebrew University of Jerusalem, 91904, Jerusalem, Israel

Supporting Information

ABSTRACT: ¹¹⁹Sn Mössbauer spectroscopy was performed on a series of formal Sn(II) dichloride and dihydride adducts bound by either carbon- or phosphorus-based electron pair donors. Upon binding electron-withdrawing metal pentacarbonyl units to the tin centers in LB·SnCl₂·M(CO)₅ (LB = Lewis base; M = Cr or W), a significant decrease in isomer shift (IS) was noted relative to the unbound Sn(II) complexes, LB·SnCl₂, consistent with removal of nonbonding s-electron density from tin upon forming Sn-M linkages (M = Cr and W). Interestingly, when the nature of the Lewis base in the series LB·SnCl₂·W(CO)₅ was altered, very little change in the IS values was noted, implying that the LB-Sn bonds were constructed with tin-based orbitals of large p-character (as supported by prior theoretical studies). In addition, variable temperature Mössbauer measurements were used to determine the mean displacement of the tin atoms in the solid state, a parameter that can be correlated with the degree of covalent bonding involving tin in these species.



INTRODUCTION

The use of Lewis basic donors to bind and concurrently stabilize reactive main group entities has been a vigorously explored concept in modern main group chemistry.¹ This strategy has enabled the study of previously inaccessible species in the condensed phase, leading to a significant advancement in knowledge with respect to chemical bonding involving inorganic elements.² Furthermore, donor-stabilization protocols have opened up new landscapes of reactivity by expanding the range of low-oxidation state main group species that can be employed as reagents.³

In line with the above-mentioned studies, we have used *N*-heterocyclic carbene (NHC) donors in conjunction with Lewis acidic acceptors to access formal low-oxidation state Group 14 methylene and ethylene complexes: NHC·EH₂·LA and NHC·H₂EE′/H₂·LA (E and E′ = Si, Ge and/or Sn; LA = Lewis acid).^{4,5} In many instances, these species were examined by combined single-crystal X-ray diffraction and theoretical density functional theory (DFT) studies; however, we were eager to obtain further data involving the tin containing analogues via Mössbauer spectroscopy. Mössbauer spectroscopy is a very useful technique for analyzing tin compounds as it gives important information regarding the degree of s-electron density at the tin center (from isomer shift, IS, values), the coordination geometry (from quadrupole splitting, QS, values), and the degree of atomic displacement of a tin center within a complex in the solid state.⁶ Consequently this paper describes the synthesis and Mössbauer spectroscopy of the new donor-acceptor adduct Cy₃P·SnCl₂·W(CO)₅, the known tin(II) amide IPr·SnCl(NHDipp)⁷ [IPr = (HCNDipp)₂C₂; Dipp = 2,6-ⁱPr₂C₆H₃], and a number of recently prepared stable

complexes of SnCl₂, SnH₂, and Cl₂SiSnCl₂ featuring *N*-heterocyclic carbene (NHC) and *N*-heterocyclic olefin donors bound to tin.^{4,8} The ultimate goal of this study is to better understand the bonding within these formally low-oxidation state Sn(II) species.

EXPERIMENTAL SECTION

General Procedures. All reactions were performed using standard Schlenk line techniques under an atmosphere of nitrogen or in an inert atmosphere glovebox (Innovative Technology, Inc.). Solvents were dried using a Grubbs-type solvent purification system⁹ manufactured by Innovative Technology, Inc., degassed (freeze-pump-thaw method) and stored under an atmosphere of nitrogen prior to use. IPr,¹⁰ (THF)₂SnCl₂W(CO)₅,¹¹ IPr·SnCl₂ (1),^{4a} IPr·SnCl₂·W(CO)₅ (2),^{4b} IPr·SnH₂·W(CO)₅ (3),^{4b} IPrCH₂·SnCl₂·W(CO)₅ (8),⁸ IPrCH₂·SnH₂·W(CO)₅ (9),⁸ IPr·SiCl₂SnCl₂·W(CO)₅ (10),^{4c} and IPr·SnCl(NHDipp) (11)⁷ were prepared according to literature procedures. Cr(CO)₆ was obtained from Aldrich and sublimed under vacuum prior to use. SnCl₂, Li[BH₄], and Cy₃P were obtained from Aldrich and used as received. ¹H, ¹³C{¹H}, and ¹¹⁹Sn NMR spectra were recorded on a Varian iNova-400 spectrometer and referenced externally to SiMe₄ (¹H, ¹³C{¹H}) and SnMe₄ (¹¹⁹Sn). Elemental analyses were performed by the Analytical and Instrumentation Laboratory at the University of Alberta. Infrared spectra were recorded on a Nicolet IR100 FTIR spectrometer as Nujol mulls between NaCl plates. Melting points were measured in sealed glass capillaries under nitrogen using a MelTemp melting point apparatus and are uncorrected.

Mössbauer Effect Spectroscopy. Temperature-dependent ^{119m}Sn Mössbauer spectra were acquired in transmission geometry

Received: March 3, 2013

Published: April 25, 2013

using a 5 mCi $^{119\text{m}}\text{Sn}$ source (CaSnO_3) as described previously.¹² All isomer shifts (IS) are relative to the centroid of a room temperature BaSnO_3 absorption spectrum, and spectrometer calibration was carried out as usual.¹³ Temperature monitoring over the extended data acquisition intervals was effected using the Daswin program of Glaberson.¹⁴ To monitor the temperature dependence of the recoil-free fraction ($-d \ln A/dT$), the transmission rate was recorded both before and after each data point acquisition.

X-ray Crystallography. Crystals of suitable quality for X-ray diffraction studies were removed from a vial in a glovebox and immediately covered with a thin layer of hydrocarbon oil (Paratone-N). A suitable crystal was selected, mounted on a glass fiber, and quickly placed in a low temperature stream of nitrogen on an X-ray diffractometer.¹⁵ All data were collected using a Bruker APEX II CCD detector/D8 diffractometer using Mo $K\alpha$ or radiation with the crystals cooled to -100°C . The data were corrected for absorption through Gaussian integration from the indexing of the crystal faces.¹⁶ Structures were solved using direct methods (SHELXS-97¹⁷ for compound 5; SIR 97¹⁸ for compound 7) or using the Patterson search/structure expansion facilities within the DIRDIF-2008 program suite²⁰ (compound 6); structure refinement was accomplished using SHELXL-97.¹⁷ The tin-bound hydrogen atoms in 6 were located in the electron difference map and refined isotropically. All carbon-bound hydrogen atoms were assigned positions based on the sp^2 or sp^3 hybridization geometries of their attached carbon atoms, and were given thermal parameters 20% greater than those of their parent atoms.

Synthetic Procedures. *Synthesis of $(\text{THF})_2\text{SnCl}_2\text{Cr}(\text{CO})_5$ (4).* To a mixture of $\text{Cr}(\text{CO})_6$ (0.50 g, 2.3 mmol) and SnCl_2 (0.43 g, 2.3 mmol) was added 85 mL of dry tetrahydrofuran (THF), and the mixture was irradiated with a 450 W mercury lamp for 6 h to give a pale orange solution. The volatiles were removed from the reaction mixture, and the product was then extracted with 30 mL of hexanes. $(\text{THF})_2\text{SnCl}_2\text{Cr}(\text{CO})_5$ was isolated as bright orange crystals by cooling the hexanes extract to -35°C . A small amount of $\text{Cr}(\text{CO})_6$ cocrystallized with the $(\text{THF})_2\text{SnCl}_2\text{Cr}(\text{CO})_5$ (as evident from $^{13}\text{C}\{^1\text{H}\}$ NMR), and a further recrystallization from hexanes was required to remove $\text{Cr}(\text{CO})_6$ and afford pure $(\text{THF})_2\text{SnCl}_2\text{Cr}(\text{CO})_5$ (0.238 g, 20%). ^1H NMR (C_6D_6): δ 1.12 (m, 4H, THF), 3.59 (m, 4H, THF). $^{13}\text{C}\{^1\text{H}\}$ NMR (C_6D_6): δ 25.2 (THF), 69.6 (THF), 215.8 (equat. CO), 222.6 (ax. CO). $^{119}\text{Sn}\{^1\text{H}\}$ NMR (C_6D_6): δ -250.1 (s). Anal. Calcd. for $\text{C}_{15}\text{H}_{16}\text{Cl}_2\text{CrO}_5\text{Sn}$: C, 29.69; H, 3.07. Found: C, 28.80; H, 2.35. Mp ($^\circ\text{C}$): 166–168.

Preparation of $\text{IPr}\text{SnCl}_2\text{Cr}(\text{CO})_5$ (5). To a mixture of IPr (0.083 g, 0.21 mmol) and $(\text{THF})_2\text{SnCl}_2\text{Cr}(\text{CO})_5$ (0.112 g, 0.213 mmol) was added 4 mL of toluene. The reaction mixture was stirred for 40 min to give a pale green slurry. The precipitate was isolated by filtration and identified as 5 (0.148 g, 91%). Crystals of 5 of suitable quality for single-crystal X-ray diffraction were grown from a toluene/hexanes mixture at -35°C . ^1H NMR (C_6D_6): δ 0.91 (d, $^3J_{\text{HH}} = 6.8$ Hz, 12H, $\text{CH}(\text{CH}_3)_2$), 1.42 (d, $^3J_{\text{HH}} = 6.8$ Hz, 12H, $\text{CH}(\text{CH}_3)_2$), 2.68 (septet, $^3J_{\text{HH}} = 6.8$ Hz, 4H, $\text{CH}(\text{CH}_3)_2$), 6.32 (s, 2H, N-CH-), 7.07 (d, $^3J_{\text{HH}} = 7.6$ Hz, 4H, ArH), 7.20 (t, $^3J_{\text{HH}} = 7.6$ Hz, 2H, ArH). $^{13}\text{C}\{^1\text{H}\}$ NMR (C_6D_6): δ 23.1 ($\text{CH}(\text{CH}_3)_2$), 25.7 ($\text{CH}(\text{CH}_3)_2$), 29.3 ($\text{CH}(\text{CH}_3)_2$), 125.2 (ArC), 126.0 (ArC), 131.9 (ArC), 132.8 (ArC), 145.4 (N-CH-), 170.9 (N-C-N), 217.1 (equat. CO), 224.5 (ax. CO). $^{119}\text{Sn}\{^1\text{H}\}$ NMR (C_6D_6): δ 165.6. IR (Nujol/ cm^{-1}): 1922 (br, νCO) and 2055 (m, νCO). Anal. Calcd. for $\text{C}_{32}\text{H}_{36}\text{Cl}_2\text{CrN}_2\text{O}_5\text{Sn}$: C, 49.90; H, 4.71; N, 3.64. Found: C, 50.15; H, 4.66; N, 3.57. Mp ($^\circ\text{C}$): 152–154.

Synthesis of $\text{IPr}\text{SnH}_2\text{Cr}(\text{CO})_5$ (6). To a mixture of 5 (0.20 g, 0.26 mmol) and $\text{Li}[\text{BH}_4]$ (12 mg, 0.55 mmol) was added 6 mL of cold (-35°C) Et_2O . The reaction mixture was warmed to room temperature and stirred for 45 min to yield a pale brown solution over a yellow precipitate. The precipitate was allowed to settle and the mother liquor was then filtered through Celite to give a beige filtrate. Removal of the volatiles from the filtrate afforded 6 as a pale beige solid (0.171 g, 94%). Crystals of suitable quality for X-ray crystallography were grown by cooling a saturated Et_2O /hexanes mixture to -35°C . ^1H NMR (C_6D_6): δ 0.89 (d, $^3J_{\text{HH}} = 6.8$ Hz, 12H, $\text{CH}(\text{CH}_3)_2$), 1.37 (d, $^3J_{\text{HH}} = 6.8$ Hz, 12H, $\text{CH}(\text{CH}_3)_2$), 2.58 (septet,

$^3J_{\text{HH}} = 6.8$ Hz, 4H, $\text{CH}(\text{CH}_3)_2$), 5.51 (s, 2H, SnH_2 , satellites: $^1J_{\text{H-}^{119}\text{Sn}} = 1180.9$ Hz; $^1J_{\text{H-}^{117}\text{Sn}} = 1128.8$ Hz), 6.47 (s, 2H, N-CH-), 7.07 (d, $^3J_{\text{HH}} = 7.6$ Hz, 4H, ArH), 7.19 (t, $^3J_{\text{HH}} = 7.6$ Hz, 2H, ArH). $^{13}\text{C}\{^1\text{H}\}$ NMR (C_6D_6): δ 22.4 ($\text{CH}(\text{CH}_3)_2$), 25.5 ($\text{CH}(\text{CH}_3)_2$), 28.8 ($\text{CH}(\text{CH}_3)_2$), 124.5 (ArC), 125.3 (ArC), 131.2 (ArC), 133.9 (ArC), 144.8 (N-CH-), 169.5 (N-C-N), 203.1 (equat. CO), 222.4 (ax. CO). $^{119}\text{Sn}\{^1\text{H}\}$ NMR (C_6D_6): δ -104.8 (s). ^{119}Sn NMR (C_6D_6): δ -106.6 (t, $^1J_{\text{H-}^{119}\text{Sn}} = 1185$ Hz, SnH_2). IR (Nujol/ cm^{-1}): 1772 (m, $\nu\text{Sn-H}$), 1882 (s, νCO) 1898 (br, νCO) and 2037 (m, νCO). Anal. Calcd. for $\text{C}_{32}\text{H}_{38}\text{CrN}_2\text{O}_5\text{Sn}$: C, 54.80; H, 5.46; N, 3.99. Found: C, 54.98; H, 5.62; N, 3.95. Mp ($^\circ\text{C}$): 136–138 (turns dark brown), 153–155 (melts).

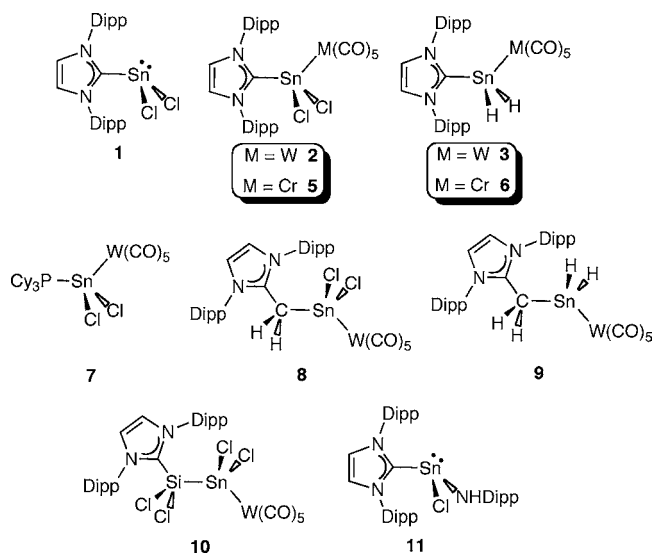
Thermolysis of $\text{IPr}\text{SnH}_2\text{Cr}(\text{CO})_5$ (6). A solution of $\text{IPr}\text{SnH}_2\text{Cr}(\text{CO})_5$ (40 mg, 0.057 mmol) in 8 mL of toluene was heated to 100°C for 36 h to obtain a green-yellow solution over a black precipitate. The solution was decanted, and the residue was extracted with 4 mL of toluene. The combined extracts were filtered through Celite, and the volatiles were removed to give a green-yellow powder (27 mg). ^1H NMR (C_6D_6) analysis of the soluble fraction revealed the presence of $\text{IPr}\text{Cr}(\text{CO})_5$ and $[(\text{HCNDipp})_2\text{CH}_2]^{4b}$ (IPrH_2) in a 35/65 mol ratio.

Independent Synthesis of $\text{IPr}\text{Cr}(\text{CO})_5$. A suspension of $\text{Cr}(\text{CO})_6$ (0.116 g, 0.527 mmol) in 25 mL of THF was irradiated with a 450 W mercury lamp for 1.5 h to give a bright orange solution of $(\text{CO})_5\text{Cr}\cdot\text{THF}$. IPr (0.204 g, 0.527 mmol) was dissolved in 10 mL of toluene and then added dropwise to the solution of $(\text{CO})_5\text{Cr}\cdot\text{THF}$. The immediate formation of a pale yellow-orange solution was observed, and the reaction mixture was stirred overnight. The volatiles were then removed under vacuum to give a pale green powder, which was further purified by recrystallization from a mixture of hexanes and toluene at -35°C (0.197 g, 64%). ^1H NMR (C_6D_6): δ 0.98 (d, $^3J_{\text{HH}} = 6.8$ Hz, 12H, $\text{CH}(\text{CH}_3)_2$), 1.38 (d, $^3J_{\text{HH}} = 6.8$ Hz, 12H, $\text{CH}(\text{CH}_3)_2$), 2.78 (septet, $^3J_{\text{HH}} = 6.8$ Hz, 4H, $\text{CH}(\text{CH}_3)_2$), 6.51 (s, 2H, N-CH-), 7.11 (d, $^3J_{\text{HH}} = 7.6$ Hz, 4H, ArH), 7.25 (t, $^3J_{\text{HH}} = 7.6$ Hz, 2H, ArH). $^{13}\text{C}\{^1\text{H}\}$ NMR (C_6D_6): δ 22.4 ($\text{CH}(\text{CH}_3)_2$), 25.6 ($\text{CH}(\text{CH}_3)_2$), 28.5 ($\text{CH}(\text{CH}_3)_2$), 124.3 (N-CH-), 125.2 (ArC), 130.8 (ArC), 137.5 (ArC), 146.2 (ArC), 200.1 (N-C-N), 216.4 (equat. CO), 220.7 (ax. CO). IR (Nujol/ cm^{-1}): 1880 (br, νCO), 1918 (br, νCO), 1981 (m, νCO), 2056 (s, νCO). Anal. Calcd. for $\text{C}_{32}\text{H}_{36}\text{N}_2\text{O}_5\text{Cr}$: C, 66.19; H, 6.25; N, 4.82. Found: C, 66.75; H, 6.18; N 4.77. Mp ($^\circ\text{C}$): 258–260.

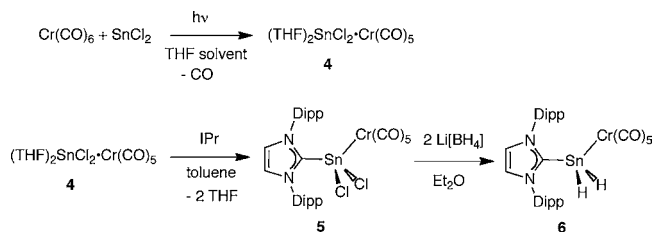
Synthesis of $\text{Cy}_3\text{P}\text{SnCl}_2\text{W}(\text{CO})_5$ (7). To a mixture of Cy_3P (0.044 g, 0.16 mmol) and $(\text{THF})_2\text{SnCl}_2\text{W}(\text{CO})_5$ (0.104 g, 0.158 mmol) was added 12 mL of toluene. The reaction mixture was stirred overnight to yield a yellow solution. The reaction mixture was then filtered, and the volatiles were then removed under vacuum to give 7 as a yellow solid (0.099 g, 79%). X-ray quality crystals were obtained by cooling a concentrated solution of 7 in toluene/hexanes to -35°C . ^1H NMR (C_6D_6): δ 1.00 (m, 9H, CyH), 1.42 (m, 9H, CyH), 1.56 (m, 6H, CyH), 1.92 (m, 6H, CyH), 2.39 (m, 3H, CyH). $^{13}\text{C}\{^1\text{H}\}$ NMR (C_6D_6): δ 25.5 (s, CyC), 27.0 (d, $^2J_{\text{C-P}} = 10.8$ Hz, CyC), 29.2 (s, CyC), 32.3 (d, $^1J_{\text{C-P}} = 14.2$ Hz, CyC), 197.2 (equat. CO) and 199.5 (ax. CO). $^{31}\text{P}\{^1\text{H}\}$ NMR (C_6D_6): δ 12.9 (with Sn and W satellites: $^2J_{\text{P-W}} = 32.5$ Hz, $^1J_{\text{P-}^{117}\text{Sn}} = 1352.2$ Hz, $^1J_{\text{P-}^{119}\text{Sn}} = 1415.3$ Hz). $^{119}\text{Sn}\{^1\text{H}\}$ NMR (C_6D_6): δ 29.4 (d, $^1J_{\text{P-}^{119}\text{Sn}} = 1413.3$ Hz). IR (Nujol, cm^{-1}): 1929 (br, νCO) and 2069 (m, νCO). Anal. Calcd. for $\text{C}_{23}\text{H}_{33}\text{Cl}_2\text{PO}_5\text{SnW}$: C, 34.79; H, 4.19. Found: C, 35.49; H, 4.19. Mp ($^\circ\text{C}$): 145–146; decomposition at 155.

RESULTS AND DISCUSSION

Synthesis of New Donor–Acceptor Adducts of SnCl_2 and SnH_2 . The compounds studied in this report by Mössbauer spectroscopy are outlined in Chart 1, and were chosen to cover a wide range of structurally distinct tin species featuring variable coordination motifs and ligating Lewis bases. While the synthesis and characterization of compounds 1–3, 8–11 have been reported in the literature,^{4,7,8} the carbene and phosphine complexes 5–7 represent new compounds, and thus relevant preparative and characterization details will be mentioned here.

Chart 1. Compounds Studied by Mössbauer Spectroscopy in this Paper

The synthetic route used to access compounds **5** and **6** is summarized in Scheme 1, and follows established procedures

Scheme 1. Synthesis of the Donor–Acceptor Complexes IPr·SnCl₂·W(CO)₅ (5**) and IPr·SnH₂·W(CO)₅ (**6**)**

for the generation of donor–acceptor complexes of stannylenes ($\text{LB}\cdot\text{R}_2\text{Sn}\cdot\text{LA}$; LB = Lewis base; LA = Lewis acid).²⁰ To begin, the synthesis of the Cr(CO)_5 adducts $\text{IPr}\cdot\text{SnCl}_2\cdot\text{Cr(CO)}_5$ (**5**) and $\text{IPr}\cdot\text{SnH}_2\cdot\text{Cr(CO)}_5$ (**6**) was motivated by a desire to compare the thermal stabilities of these species with the previously known W(CO)_5 -capped complexes **2** and **3**.^{4b} Moreover, it was anticipated that there would be an increase in the ¹¹⁹Sn Mössbauer sensitivity of the Cr(CO)_5 complexes **5** and **6** because of the lighter nature of the Cr center which generally reduces nonresonant scattering relative to W, leading to an enhancement of the Mössbauer effect.²¹ As shown in Scheme 1, the requisite stannylenes reagent $(\text{THF})_2\text{SnCl}_2\cdot\text{Cr(CO)}_5$ (**4**) was generated¹¹ by the photolysis of Cr(CO)_6 in the presence of SnCl_2 in THF, and isolated as orange crystals in a low yield of 20% after recrystallization from hexanes; an additional recrystallization step from hexanes was required to separate **4** from residual Cr(CO)_6 . The donor–acceptor complex $\text{IPr}\cdot\text{SnCl}_2\cdot\text{Cr(CO)}_5$ (**5**) was then formed in high yield (91%) by exchanging the labile THF donors in **4** with the *N*-heterocyclic carbene, IPr. Conversion of the Sn(II) dichloride adduct **5** into the dihydride analogue $\text{IPr}\cdot\text{SnH}_2\cdot\text{Cr(CO)}_5$ (**6**) was accomplished by combining $\text{IPr}\cdot\text{SnCl}_2\cdot\text{Cr(CO)}_5$ (**5**) with 2 equiv of $\text{Li[BH}_4\text{]}$. Both the Cr(CO)_5 adducts **5** and **6** were characterized by single-crystal X-ray crystallography, and the refined structures are presented in Figures 1 and 2,

respectively, with relevant crystallographic data summarized in Table 1.

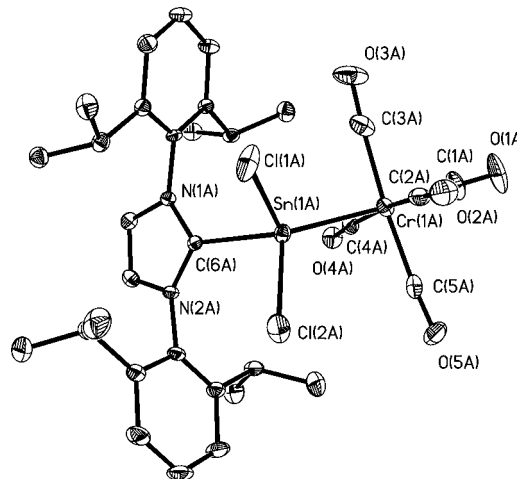


Figure 1. Thermal ellipsoid (30% probability level) plot of $\text{IPr}\cdot\text{SnCl}_2\cdot\text{Cr(CO)}_5$ (**5**). All hydrogen atoms and hexane solvate have been omitted for clarity; only one molecule of the three in the asymmetric unit is shown. Selected bond lengths [Å] and angles [deg]: *Molecule A*: Sn–Cr 2.5805(8), Sn–C(6) 2.270(4), Sn–Cl(1) 2.3864(13), Sn–Cl(2) 2.3640(12), Cr–C(1) 1.862(5), Cr–C(2–5) 1.886(5) to 1.905(5); C(6)–Sn–Cr 127.40(10), Sn–Cr–C(1) 177.50(19), Sn–Cr–C(2–5) 86.91(15) to 93.53(14). *Molecule B*: Sn–Cr 2.5825(8), Sn–C(6) 2.256(4), Sn–Cl(1) 2.3786(12), Sn–Cl(2) 2.3742(12), Cr–C(1) 1.857(5), Cr–C(2–5) 1.878(5) to 1.905(6); C(6)–Sn–Cr 127.21(10), Sn–Cr–C(1) 177.7(2), Sn–Cr–C(2–5) 86.98(14) to 93.55(15). *Molecule C*: Sn–Cr 2.5678(8), Sn–C(6) 2.258(4), Sn–Cl(1) 2.3620(13), Sn–Cl(2) 2.3693(15), Cr–C(1) 1.853(6), Cr–C(2–5) 1.860(7) to 1.916(7); C(6)–Sn–Cr 127.22(10), Sn–Cr–C(1) 176.0(3), Sn–Cr–C(2–5) 87.22(16) to 94.47(19).

The successful crystallization of $\text{IPr}\cdot\text{SnCl}_2\cdot\text{Cr(CO)}_5$ (**5**) has added importance to the current study with regard to interpretation of the Mössbauer data as the related tungsten

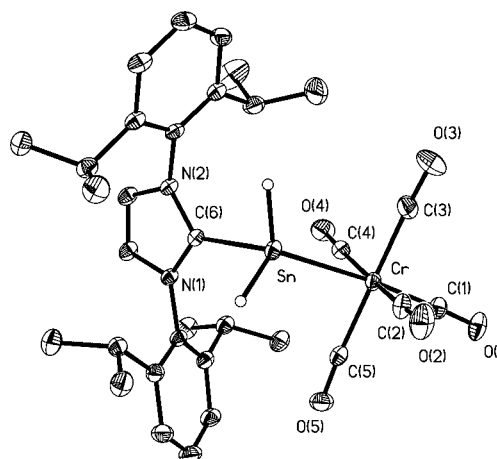


Figure 2. Thermal ellipsoid (30% probability level) plot of $\text{IPr}\cdot\text{SnH}_2\cdot\text{Cr(CO)}_5$ (**6**). Carbon-bound hydrogen atoms and hexane solvate have been omitted for clarity. Selected bond lengths [Å] and angles [deg]: Sn–Cr 2.6247(3), Sn–C(6) 2.2358(15), Sn–H 1.59(3) and 1.67(2), Cr–C(1) 1.8347(19), Cr–C(2–5) 1.870(2) to 1.8965(19); C(6)–Sn–Cr 118.69(4), Sn–Cr–C(1) 175.36(6), Sn–Cr–C(2–5) 85.49(6) to 91.03(7)

Table 1. Crystallographic Data for Compounds 5–7

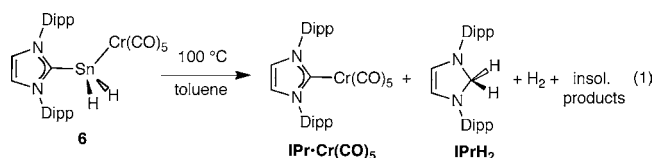
	5	6	7
empirical formula	C ₃₂ H ₃₆ Cl ₂ CrN ₂ O ₅ Sn	C ₃₅ H ₄₅ CrN ₂ O ₅ Sn	C ₂₃ H ₃₃ Cl ₂ O ₅ PSnW
fw	770.22	744.42	793.90
cryst dimens (mm ³)	0.37 × 0.36 × 0.05	0.54 × 0.37 × 0.20	0.24 × 0.24 × 0.12
cryst syst	monoclinic	monoclinic	monoclinic
space group	P2 ₁ /n	P2 ₁ /n	P2 ₁ /n
unit cell dimensions			
a (Å)	10.5962(6)	10.8773(5)	12.4381(8)
b (Å)	18.9655(11)	20.1714(9)	17.4207(11)
c (Å)	51.458(3)	16.8178(7)	14.3204(9)
α (deg)	90	90	90
β (deg)	91.5446(7)	103.0007(5)	113.6615(6)
γ (deg)	90	90	90
V (Å ³)	10337.3(10)	3595.4(3)	2842.1(3)
Z	12	4	4
ρ (g cm ⁻³)	1.485	1.375	1.855
abs coeff (mm ⁻¹)	1.235	1.037	5.197
T (K)	173(1)	173(1)	173(1)
2θ _{max} (deg)	52.86	55.10	55.32
total data	82030	31765	25198
unique data (R _{int})	21256 (0.0642)	8260 (0.0184)	6598 (0.0182)
obs data [I > 2σ(I)]	13968	7417	5972
params	1162	405	298
R ₁ [I > 2σ(I)] ^a	0.0451	0.0221	0.0196
wR ₂ [all data] ^a	0.0976	0.0634	0.0490
max/min Δρ (e ⁻ Å ⁻³)	1.163/-1.106	0.329/-0.459	2.072/-0.833

$$^a R_1 = \frac{\sum ||F_o| - |F_c||}{\sum |F_o|}; wR_2 = \left[\frac{\sum w(F_o^2 - F_c^2)^2}{\sum w(F_o^4)} \right]^{1/2}.$$

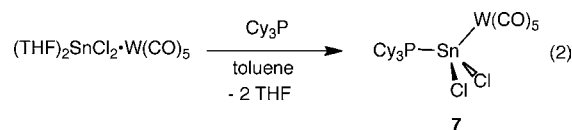
congener, IPr·SnCl₂·W(CO)₅ (**2**),^{4b} did not yield satisfactory crystallographic data for structure refinement; notably, NMR and IR spectroscopy suggest that these two SnCl₂ complexes have similar overall geometries. An average C_{IPr}-Sn distance of 2.261(7) Å is found in the solid state structure of **5** (three molecules in the asymmetric unit), and is shorter than the corresponding C_{IPr}-Sn bond length of 2.341(8) Å in IPr·SnCl₂ (**1**);^{4a} the C–Sn bond contraction in **5** relative to that in compound **1** is a likely reflection of the electron withdrawing character of the Cr(CO)₅ group which enhances the Lewis acidity of the SnCl₂ unit, leading to a stronger carbene carbon–tin dative interaction.²² The C_{IPr}-Sn bond length in the hydrido analogue IPr·SnH₂·Cr(CO)₅ (**6**) is 2.2358(15) Å and similar to that found in **5**; the hydrogen atoms bound to tin were located in the electron difference map and refined isotropically to yield an average Sn–H distance of 1.63(4) Å.

NMR spectroscopy corroborated the presence of a SnH₂ unit in **6** as a triplet resonance at –106.6 ppm was observed in the ¹¹⁹Sn NMR spectrum with a Sn–H coupling constant (¹J_{119Sn–H}) of 1185 Hz. For comparison, an upfield shifted triplet at –309 ppm (¹J_{119Sn–H} = 1158 Hz) was previously noted in the ¹¹⁹Sn NMR spectrum of IPr·SnH₂·W(CO)₅ (**3**).^{4b} Moreover, a Sn–H stretching band can be identified in the IR spectrum of **6** [$\nu = 1772 \text{ cm}^{-1}$] which is in the same spectral region as the Sn–H vibrations in the W(CO)₅ adduct **3** (1786 cm⁻¹). IPr·SnH₂·Cr(CO)₅ (**6**) is stable for indefinite periods of time in arene solvents or in the solid state, with signs of decomposition evident upon heating a solid sample to about 136 °C under nitrogen. When a sample of **6** was heated in toluene to 100 °C for 36 h the formation of a black precipitate along with the presence of IPr·Cr(CO)₅ and IPrH₂ in solution (35/65 ratio by ¹H NMR spectroscopy) was noted (eq 1); the identity of the IPr·Cr(CO)₅ product was confirmed via an

independent synthesis of this species from IPr and THF·Cr(CO)₅.



As part of our general program geared toward stabilizing reactive main group hydrides, such as the methylene analogues EH₂ (E = Si–Sn),^{4,8} the synthesis of various Sn(II) dichloride adducts featuring noncarbene donor ligands was explored as precursors to the desired SnH₂ complexes (eq 2). The attempted conversion of the new phosphine-capped adduct Cy₃P·SnCl₂·W(CO)₅ (**7**) (eq 2) to its dihydride analogue will be the focus of another publication; however for the purpose of Mössbauer spectroscopic analysis, this species represents a useful structural analogue to its carbene and N-heterocyclic olefin (IPrCH₂) coordinated counterparts (**1–6** and **8–10**). The target donor–acceptor stannylene adducts Cy₃P·SnCl₂·W(CO)₅ (**7**) was obtained in high yield as an air- and moisture-sensitive yellow solid by treating the known Sn–W precursor, (THF)₂SnCl₂·W(CO)₅,¹¹ with tricyclohexylphosphine in toluene (eq 2); Cy₃P·SnCl₂·W(CO)₅ (**7**) was also further characterized by single-crystal X-ray crystallography (Figure 3).



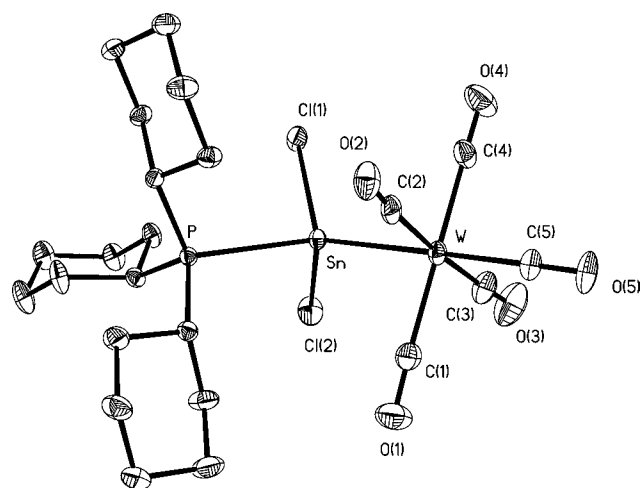


Figure 3. Thermal ellipsoid plot (30% probability level) of $C_3P \cdot SnCl_2 \cdot W(CO)_5$ (**7**) with hydrogen atoms omitted for clarity. Selected bond lengths [Å] and angles [deg]: Sn–W 2.7438(2), Sn–P 2.6330(6), Sn–Cl(1) 2.3848(7), Sn–Cl(2) 2.3858(8), W–C(5) 1.983(3), W–C(1–4) 2.023(3) to 2.047(4); P–Sn–W 126.707(15), Cl(1)–Sn–Cl(2) 99.69(3), Sn–W–C(5) 177.98(8), Sn–W–C(1–4) 88.52(8) to 91.80(7).

The tricyclohexylphosphine-appended stannylene complex $C_3P \cdot SnCl_2 \cdot W(CO)_5$ (**7**) yields a highly informative $^{31}P\{^1H\}$ NMR spectrum with a primary resonance at 12.9 ppm accompanied by satellite doublet resonances due to coupling of phosphorus to both NMR active ^{117}Sn and ^{119}Sn nuclei ($I = 1/2$; $^1J_{P-^{117}Sn} = 1325.2$ Hz, $^1J_{P-^{119}Sn} = 1415.3$ Hz); the ratio of these coupling constants also matched the expected value based upon the gyromagnetic ratio of the ^{117}Sn and ^{119}Sn nuclei. An additional doublet satellite feature is also present in the $^{31}P\{^1H\}$ NMR spectrum of **7** resulting from the coupling between phosphorus and NMR active ^{183}W nuclei ($I = 1/2$; 14% abundance; $^2J_{P-W} = 32.5$ Hz). Confirmation of P–Sn–W atomic connectivity in **7** was obtained via single-crystal X-ray crystallography with the refined structure presented in Figure 3.

Compound **7** contains a distorted tetrahedral coordination environment at tin [P–Sn–W angle = 126.707(15)°; Cl(1)–Sn–Cl(2) angle = 99.69(3)°] with a Sn–P distance of 2.6330(6) Å. This Sn–P interaction can be compared to related compounds with formally dative P→Sn bonding [e.g., in $Me_3P \cdot SnCl_4 \cdot PMe_3$ the Sn–P distances were found to be 2.5654(7) Å].²³

Mössbauer Spectroscopy of Stannylenes, $SnCl_2$ and SnH_2 , Supported Solely by a Lewis Base or Concurrently by a Lewis Base and Acid (Donor–Acceptor Coordination). A primary theme of the current study is to gather ^{119}Sn Mössbauer spectroscopic data for various stannylene complexes to gain insight into the bonding/coordination environments at the tin centers. The discussion of these data will occur in two parts: (a) discussion of the isomer shift (IS) and quadrupole splitting (QS) parameters obtained, (b) presentation and analysis of variable temperature Mössbauer data including the determination of the root-mean-square-amplitude-of-vibration (rmsav) for the tin centers. As expected, the resonance spectra of Sn(II) compounds generally evidence two absorption maxima indicative of a well-resolved quadrupole hyperfine interaction (QS). In many Sn(II) species, a major contribution to this QS is due to the presence of the nonbonding pair of electrons, which creates considerable asymmetry in the

electronic field gradient about tin. A representative spectrum of $IPr \cdot SnCl_2$ (**1**) is shown to highlight this spectroscopic feature (Figure 4).

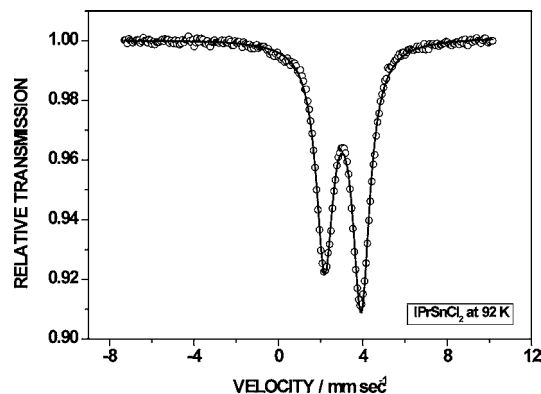


Figure 4. Mössbauer spectrum of $IPr \cdot SnCl_2$ (**1**) recorded at 92 K.

Low-Temperature Mössbauer Data Including the Determination of Isomer Shift (IS) and Quadrupole Splitting (QS) Values.

As discussed in the Introduction, the isomer shift (IS) of a tin compound provides a means to estimate the *s*-electron density that resides in close proximity to a tin nucleus with high IS values (e.g., 2.6–4 $mm\ s^{-1}$) indicative of Sn(II) centers with significant nonbonding *s*-electron density.^{2d,6,24} Upon oxidation of tin to its maximal +4 state, *s*-electron density is effectively removed from the tin center resulting in a decrease in IS to near zero values, with $BaSnO_3$ taken as a reference with IS = 0 $mm\ s^{-1}$. Therefore changes in IS values should track well with changes in *s*-electron density at tin. Table 2 contains the IS and QS values obtained at temperatures near 90 K for the tin species outlined in Chart 1.

The first compound to be investigated by Mössbauer spectroscopy among the compounds in Chart 1 was the *N*-heterocyclic carbene adduct $IPr \cdot SnCl_2$ (**1**), which contains a formal Sn(II) center datively bound by a carbene donor. This

Table 2. Isomer Shift (IS) and Quadrupole Splitting (QS) Data for Compounds 1–3, 5–11

compound	isomer shift ($mm\ s^{-1}$)	quadrupole splitting ($mm\ s^{-1}$)
$IPr \cdot SnCl_2$ (1)	3.062(8)	1.732(8)
$IPr \cdot SnCl_2 \cdot W(CO)_5$ (2)	1.962(50)	2.105(15)
$IPr \cdot SnH_2 \cdot W(CO)_5$ (3)	1.667(7)	2.302(8)
$IPr \cdot SnCl_2 \cdot Cr(CO)_5$ (5)	1.951(27)	1.974(6)
$IPr \cdot SnH_2 \cdot Cr(CO)_5$ (6)	1.644(3)	2.717(61)
$Cy_3P \cdot SnCl_2 \cdot W(CO)_5$ (7)	2.099(3)	2.076(3)
$IPrCH_2 \cdot SnCl_2 \cdot W(CO)_5$ (8) ^a	1.846(41)	2.357(16)
	2.150(6)	2.41(11) ^b
$IPrCH_2 \cdot SnH_2 \cdot W(CO)_5$ (9)	1.807(3)	1.909(3)
$IPr \cdot Cl_2Si \cdot SnCl_2 \cdot W(CO)_5$ (10)	2.053(22)	2.427(22)
$IPr \cdot SnCl(NHDipp)$ (11)	2.809(8)	2.238(8)

^aTwo crystallographically distinct tin sites in **8** was also noted by single crystal X-ray diffraction (modeled with 0.4 and 0.6 occupancy factors, respectively);⁷ a 1:1 ratio between the two sites was determined via Mössbauer spectral fitting. ^bThe larger error associated with this QS value is due to the low receptivity of this tin site to the Mössbauer effect (2.23% at 92.2 K).

species yields a well-defined doublet resonance centered at an isomer shift value of 3.062(8) mm s⁻¹ (Figure 4). This value is very close to that observed in the bis(amido)-naphthylstannylylene :Sn[(ⁱPrN)₂C₁₀H₆] (C₁₀H₆ = 1,8-naphthyl) [2.913(3) mm s⁻¹],²⁵ adding support for the presence of a Sn(II) site with a nonbonding lone pair in **1**. The structurally related three-coordinate Sn(II) adduct IPr·SnCl(NHDipp) (**11**) was also studied by Mössbauer spectroscopy and yields a slightly lower IS value of 2.809(8) mm s⁻¹ relative to **1**. Prior single-crystal X-ray diffraction studies reveal that both **1** and **11** have similar coordination modes at tin with pyramidalized Sn centers consistent with the presence of a stereochemically active lone pair. Specifically, equivalent bond angle sum values at each Sn center were found [$\sum_{\text{Sn}} = 280.0(3)^\circ$ for **1**; $\sum_{\text{Sn}} = 279.63(13)^\circ$ for **11**]^{4a,7} suggesting that a similar hybridization scheme (and s-electron density at tin) is present in each compound, thus providing a rationale for the similar IS values in both species. The structurally related Sn(II) anion, [SnCl₃]⁻, afforded an IS value of 3.45(2) mm s⁻¹ (in [SnCl(18-crown-6)][SnCl₃]) with a quadrupole splitting value, 0.89(2) mm s⁻¹,^{2b,26} that is expectedly smaller than the QS values found in either compounds **1** and **11** because of the presence of three equivalent chloride groups at tin in the [SnCl₃]⁻ anion.

Upon ligation of the electron withdrawing Cr(CO)₅ and W(CO)₅ groups onto the IPr·SnCl₂ unit to form Sn–Cr and Sn–W bonds, there is a noticeable change in the IS and QS values obtained. For example, both IPr·SnCl₂·W(CO)₅ (**2**) and IPr·SnCl₂·Cr(CO)₅ (**5**) exhibit significant decreases in IS values of about 1.1 mm s⁻¹ compared to IPr·SnCl₂ (**1**) [IS = 1.962(50) and 1.951(27) mm s⁻¹, for **2** and **5**, respectively], indicating that substantial removal of s-electron density from the tin center in **1** occurs upon binding the Lewis acids Cr(CO)₅ and W(CO)₅. Prior calculations on the model complex ImMe₂·SnH₂·W(CO)₅ [ImMe₂ = (HCNMe)₂C:] shed some light on this effect as the Sn–W interaction was considerably covalent [62% contribution from Sn; 38% from W] with a tin orbital of significant s-character (63%) used to make the Sn–W bond.^{4b} These calculations are in line with the reduction in s-electron density at Sn upon coordination to the Lewis acidic M(CO)₅ group (M = Cr and W) to the IPr·SnCl₂ unit. Replacement of the chloride groups in **2** and **5** with hydrides (to give IPr·SnH₂·M(CO)₅; M = Cr and W; **3** and **6**) consistently affords a decrease in IS value by about 0.3 mm s⁻¹. One possible contributing factor for this effect is derived from Bent's rule,²⁷ which states that orbitals with more p-character (and concurrently less s-character) are used to bind electronegative elements. Therefore when the electronegative Cl atoms in **2** and **5** are replaced by the less electronegative H atoms, the resulting Sn–H bonds are expected to have more s-orbital contribution from Sn, and thus a lower IS value occurs as more s-electron density at tin is being pulled away to form covalent bonds. The increase in QS values in the SnH₂ analogues relative to the SnCl₂ derivatives was somewhat surprising given that the presence of hydride groups generally leads to lower QS values relative to their organo- and halide-substituted counterparts. For example, the QS value for the tetravalent tin center in ArSnSnH₂Ar was found to be 0.967(4) mm s⁻¹²⁸ while in the methyl-substituted species, ArSnSnMe₂Ar,²⁹ a value of 0.32(1) mm s⁻¹ was noted (Ar = terphenyl ligands). In this connection it is appropriate to note an unexpected observation made in the early days of ¹¹⁹Sn Mössbauer effect spectroscopy,³⁰ namely, that when the metal atom is ligated only to nearest neighbor atoms which do not

have lone pair bonding electrons, but which clearly do not have cubic (i.e., T_d or O_h) symmetry, such as Ph₃SnH or PhSnMe₃, the QS interaction becomes too small to resolve from the spectral data.³⁰ In the present cases however, the presence of the W(CO)₅ group in **3** and **9**, or Cr(CO)₅ in **6** results in a significant electric field gradient at the Sn center, leading to well resolved QS interactions in the respective Mössbauer effect spectra (despite the simultaneous presence of two H atoms in the structures).

A series of complexes containing the formal electron pair donor, IPrCH₂, were also analyzed by Mössbauer spectroscopy. Interestingly, the chloro derivative IPrCH₂·SnCl₂·W(CO)₅ (**8**) gave two closely spaced doublet resonances with IS values of 1.846(41) and 2.150(6) mm s⁻¹, suggesting the presence of two slightly different Sn environments in the solid state. This observation is corroborated by the X-ray diffraction data which yields two sets of U_{eq} values for the Sn center in **8** with refined site occupancies of 0.6 to 0.4.⁷ Upon conversion of **8** to the dihydride IPrCH₂·SnH₂·W(CO)₅ (**9**), an overall reduction in isomer shift is observed [IS = 1.807(3) mm s⁻¹], which mirrors the trends noted in the IPr coordinated tin complexes. Theoretical Natural Bond Orbital (NBO) analysis of the model complex ImMe₂CH₂·SnH₂·W(CO)₅ (B3LYP/cc-pVDZ) reveals that an orbital of similar hybridization at tin is used to form the Sn–W linkage as in ImMe₂·SnH₂·W(CO)₅ (61% s-character at tin);^{4b,7} however, the Sn–W bond in the ImMe₂CH₂ is appreciably more polar with a 82% electron density participation from Sn versus 62% in ImMe₂·SnH₂·W(CO)₅.⁷ In both of the ImMe₂ and ImMe₂CH₂ models, the tin centers form dative Sn–C interactions with orbitals that are predominantly (>85%) p-orbital in character.

To further investigate the role of the donor on the electronic environment about the formal Sn(II) sites in the complexes LB·SnCl₂·W(CO)₅ (LB = Lewis base), a Mössbauer spectrum was obtained for the phosphine adduct Cy₃P·SnCl₂·W(CO)₅ (**7**). The Cy₃P adduct **7** yields an isomer shift value of 2.099(3) mm s⁻¹ with corresponding quadrupole splitting of 2.076(3) mm s⁻¹. The isomer shift value for **7** is quite similar to those observed in the IPr and IPrCH₂-substituted dichlorostannylylene complexes IPr·SnCl₂·W(CO)₅ (**3**) and IPrCH₂·SnCl₂·W(CO)₅ (**9**); thus despite what appears to be significant changes in donor type, the degree of s-electron density at the tin centers in these species remains largely invariant. A similar effect was noted within the series THF·Sn^tBu₂·Cr(CO)₅, DMSO·Sn^tBu₂·Cr(CO)₅, and DMAP·Sn^tBu₂·Cr(CO)₅ wherein a narrow IS range of 1.98(6)–2.11(6) mm s⁻¹ was observed.³¹ Interestingly, the silastannene adduct IPr·Cl₂SiSnCl₂·W(CO)₅ (**10**) also gave a doublet Mössbauer resonance with an isomer shift of ~2 mm s⁻¹ [2.053(22) mm s⁻¹] (Figure 5). The nature of the bonding in **10** will be the subject of a future detailed theoretical study; however one can represent the bonding in this species with various canonical forms (Scheme 2) including one where the IPr·SiCl₂ unit acts as a Lewis base, and forms a dative Si–Sn interaction with the SnCl₂·W(CO)₅ array. Calculations on the model species ImMe₂·H₂SiSnH₂·W(CO)₅ show that the Si–Sn bond is largely made up of an orbital on tin with very large p-character (85%),^{4d} which mirrors the hybridization scheme calculated for the C_{IPr}-Sn interaction in ImMe₂·SnH₂·W(CO)₅.^{4b} These initial theoretical studies support the observation that the IS values in the complexes LB·SnCl₂·W(CO)₅ studied here (LB = IPr, IPrCH₂, Cy₃P, and IPr·SiCl₂) remain relatively similar upon changing the Lewis

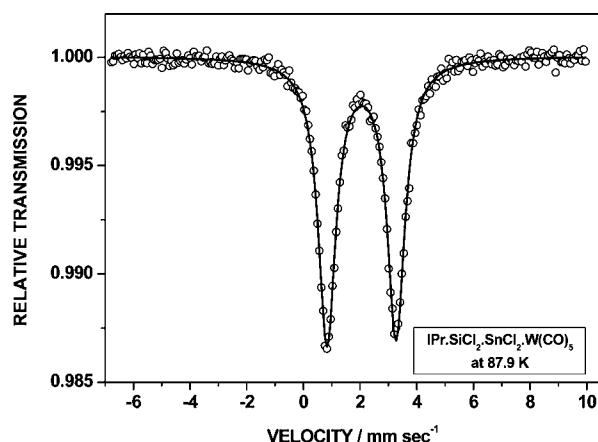
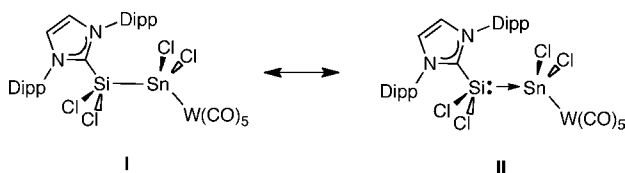


Figure 5. Mössbauer spectrum of $\text{IPr}\cdot\text{Cl}_2\text{SiSnCl}_2\cdot\text{W}(\text{CO})_5$ (10) recorded at 88 K.

Scheme 2. Possible Canonical Forms Illustrating the Si–Sn Bonding in $\text{IPr}\cdot\text{Cl}_2\text{SiSnCl}_2\cdot\text{W}(\text{CO})_5$ (10)



base as the LB–Sn bonds do not involve high *s*-orbital character at tin.

One particularly noteworthy observation is that quadrupole hyperfine splitting appears to increase upon binding of a Lewis acidic $\text{M}(\text{CO})_5$ unit to tin ($\text{M} = \text{Cr}$ and W); for example, the QS value increases significantly on conversion of $\text{IPr}\cdot\text{SnCl}_2$ (1) [$1.732(8) \text{ mm s}^{-1}$] to $\text{IPr}\cdot\text{SnCl}_2\cdot\text{W}(\text{CO})_5$ (3) [$2.105(15) \text{ mm s}^{-1}$]. For reference, a similar increase in QS value was noted upon coordinating a $\text{W}(\text{CO})_5$ group to the lone pair on tin in $\text{Sn}(\text{acac})_2$ [QS for $\text{Sn}(\text{acac})_2 = 1.89 \text{ mm s}^{-1}$ vs QS for $(\text{CO})_5\text{W}\cdot\text{Sn}(\text{acac})_2 = 2.35 \text{ mm s}^{-1}$].³² These changes in QS parameters can be rationalized by the removal of electron density from tin-based orbitals that are primarily of *s*-character to form a new Sn–W bonds, which in turn increases the relative occupation of orbitals of increased *p*-character at tin; this effect is known to create increased asymmetry in the electric field gradient at tin and yield higher QS values.²⁴

Variable Temperature Mössbauer Experiments and Tin Atom Dynamics in Selected Donor-bound Sn(II) Complexes. It is appropriate at this stage to comment on the metal atom dynamics in these compounds, for which single-crystal X-ray data are available. As shown in previous studies,^{13,33} the temperature dependence of the root-mean-square-amplitude of-vibration (rmsav) can be extracted from both the Mössbauer studies as well as the U_{ij} values derived from the X-ray data. The rmsav can be derived from the Mössbauer parameter \mathcal{F} , as given by $\mathcal{F} = -k^2 \langle x_{\text{ave}}^2 \rangle$ where k is the wave vector of the 23.9 keV gamma ray, and $\langle x_{\text{ave}}^2 \rangle^{1/2}$ is the rmsav value. A typical comparison between the value of \mathcal{F} extracted from Mössbauer data and that obtained from single-crystal X-ray crystallography is shown graphically for $\text{Cy}_3\text{P}\cdot\text{SnCl}_2\cdot\text{W}(\text{CO})_5$ (7) in Figure 6; similar calculated rmsav values were observed for compounds 5 and 11 (as summarized in Table 3). In each of these three cases (compounds 5, 7, and 11) the Mössbauer \mathcal{F} values are smaller than the X-ray derived

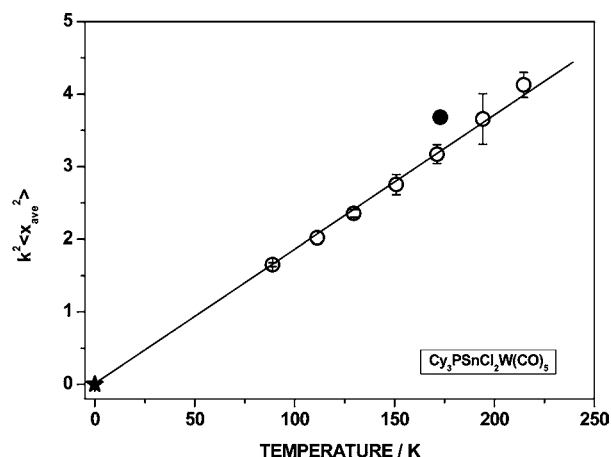


Figure 6. The \mathcal{F} parameters for $\text{Cy}_3\text{P}\cdot\text{SnCl}_2\cdot\text{W}(\text{CO})_5$ (7) as a function of temperature. The starred data point is the extrapolation of the high temperature regime data to $T = 0$, making the assumption that the zero point motion contribution to the data in the range $90 < T < 225 \text{ K}$ is negligibly small. The filled data point represents the \mathcal{F} parameter at 173 K taken from the single crystal X-ray data.

value at the temperature of the latter determination. As noted previously,³³ this observation can be rationalized for cases where the Sn atom is ligated to its nearest neighbor environment by one or more σ bonds. In such an environment low frequency librational or torsional modes contribute to the U_{ij} in the X-ray data, but to which the Mössbauer technique is very much less sensitive.

CONCLUSION

A series of complexes containing tin centers in formal +2 oxidation states were studied at low temperatures by Mössbauer spectroscopy. In the case of the tin(II) compounds $\text{IPr}\cdot\text{SnX}_2$ ($\text{X} = \text{Cl}$ or Cl and NHDipp) isomer shift values typical for Sn(II) compounds with a stereochemically active lone pair are obtained. When these lone pairs are bound to Lewis acidic $\text{M}(\text{CO})_5$ units ($\text{M} = \text{Cr}$ and W), significant nonbonding (lone pair) *s*-electron density is pulled away from the tin center to form new Sn–M linkages, resulting in a concomitant decrease in IS value of about 0.3 mm s^{-1} . Despite the decrease in IS values, the bonding and reactivity of these species, $\text{LB}\cdot\text{SnCl}_2\cdot\text{W}(\text{CO})_5$, still suggest that a Sn(II) oxidation state is an appropriate descriptor with dative LB–Sn bonds present (LB = Lewis base). From detailed Mössbauer studies involving many four-coordinate tin complexes $\text{LB}\cdot\text{SnCl}_2\cdot\text{W}(\text{CO})_5$, it was shown that the isomer shift values (and *s*-electron density at tin) were largely invariant of the nature of the Lewis base coordinated to tin (LB = IPr , IPrCH_2 , Cy_3P , and $\text{IPr}\cdot\text{SiCl}_2$). This result suggests that the terminal dative LB–Sn interactions in these adducts involve tin based orbitals of similar *s*-character, and preliminary theoretical analyses point toward LB–Sn bonding interactions derived from Sn-based orbitals of large *p*-character (>85%), thus partially explaining the lack of significant IS deviations across this compound series. Variable temperature experiments were recorded on selected tin complexes, and these data showed that the Sn centers in each of the molecular classes were found in significantly covalent bonding environments. These interactions lead to added low frequency librational or torsional modes that are more sensitive to the single-crystal X-ray diffraction studies versus Mössbauer data,

Table 3. Variable Temperature Root-Mean-Square-Amplitude-of-Vibration (rmsav) of the Metal Atom in Compounds 5, 7, and 11^a

temperature (K)	compound 5	compound 7	compound 11
	IPr-SnCl ₂ ·Cr(CO) ₅	Cy ₃ P-SnCl ₂ ·W(CO) ₅	IPr-SnCl(NHDipp)
100	0.114	0.113	0.123
125	0.127	0.127	0.138
150	0.140	0.139	0.151
175	0.151	0.151	0.163
200	0.161	0.161	0.174
225	0.171	0.172	0.185

^aThe rmsav values are given in Å with experimental uncertainties of about 10%.

resulting in deviations in the root-mean-square-amplitude-of-vibration (rmsav) values extracted by the two methods.

■ ASSOCIATED CONTENT

■ Supporting Information

Mössbauer spectra for compounds 2–9 and 11, and variable temperature Mössbauer data for compounds 5 and 11. This material is available free of charge via the Internet at <http://pubs.acs.org>.

■ AUTHOR INFORMATION

Corresponding Author

*E-mail: rolfe.herber@mail.huji.ac.il (R.H.H.), erivard@ualberta.ca (E.R.).

Notes

The authors declare no competing financial interest.

■ ACKNOWLEDGMENTS

This work was supported by the Natural Sciences and Engineering Research Council (NSERC) of Canada (Discovery Grant for E.R.; Undergraduate Research Award for S.M.M.), the Canada Foundation for Innovation (CFI), Alberta Innovates-Technologies Futures (New Faculty Award to E.R.; Graduate Award to S.M.I.A.). The authors are also indebted to Prof. I. Nowik for detailed discussions of the Mössbauer data reported here.

■ REFERENCES

- (1) For selected review articles, see: (a) Kuhn, N.; Al-Sheikh, A. *Coord. Chem. Rev.* **2005**, *249*, 829. (b) Jones, C. *Chem. Commun.* **2001**, 2293. (c) Wang, Y.; Robinson, G. H. *Inorg. Chem.* **2011**, *50*, 12326. (d) Yao, S.; Xiong, Y.; Driess, M. *Organometallics* **2011**, *30*, 1748. (e) Martin, D.; Melaimi, M.; Soleilhavoup, M.; Bertrand, G. *Organometallics* **2011**, *30*, 5304.
- (2) Recent examples highlighting this concept include: (a) Braunschweig, H.; Dewhurst, R. D.; Hammond, K.; Mies, J.; Radacki, K.; Vargas, A. *Science* **2012**, *336*, 1420. (b) Kinjo, R.; Donnadiou, B.; Ali Celik, M.; Frenking, G.; Bertrand, G. *Science* **2011**, *333*, 610. (c) Jones, C.; Sidiropoulos, A.; Holzmann, N.; Frenking, G.; Stasch, A. *Chem. Commun.* **2012**, *48*, 9855. (d) Macdonald, C. L. B.; Bandyopadhyay, R.; Cooper, B. F. T.; Friedl, W. W.; Rossini, A. J.; Schurko, R. W.; Eichhorn, S. H.; Herber, R. H. *J. Am. Chem. Soc.* **2012**, *134*, 4332. (e) Chitnis, S. S.; Burford, N.; Ferguson, M. J. *Angew. Chem., Int. Ed.* **2013**, *52*, 2042. (f) Chandra Mandal, K.; Roesky, H. W.; Schwarzer, M. C.; Frenking, G.; Niepötter, B.; Wolf, H.; Herbst-Irmer, R.; Stalke, D. *Angew. Chem., Int. Ed.* **2013**, *52*, 2963.
- (3) (a) Filippou, A. C.; Chernov, O.; Stumpf, K. W.; Schnakenburg, G. *Angew. Chem., Int. Ed.* **2010**, *49*, 3296. (b) Xiong, Y.; Yao, S.; Müller, R.; Kaupp, M.; Driess, M. *Nat. Chem.* **2010**, *2*, 577. (c) Ghadwal, R. S.; Roesky, H. W.; Pröpper, K.; Dittrich, B.; Klein,

S.; Frenking, G. *Angew. Chem., Int. Ed.* **2011**, *50*, 5374. (d) Cui, H.; Ma, B.; Cui, C. *Organometallics* **2012**, *31*, 7339.

(4) (a) Thimer, K. C.; Al-Rafia, S. M. I.; Ferguson, M. J.; McDonald, R.; Rivard, E. *Chem. Commun.* **2009**, 7119. (b) Al-Rafia, S. M. I.; Malcolm, A. C.; Liew, S. K.; Ferguson, M. J.; Rivard, E. *J. Am. Chem. Soc.* **2011**, *133*, 777. (c) Al-Rafia, S. M. I.; Malcolm, A. C.; McDonald, R.; Ferguson, M. J.; Rivard, E. *Angew. Chem., Int. Ed.* **2011**, *50*, 8354. (d) Al-Rafia, S. M. I.; Malcolm, A. C.; McDonald, R.; Ferguson, M. J.; Rivard, E. *Chem. Commun.* **2012**, *48*, 1308.

(5) For related studies on low-oxidation state heavy group 14 element hydrides, see: (a) Eichler, B. E.; Power, P. P. *J. Am. Chem. Soc.* **2000**, *122*, 8785. (b) Richards, A. F.; Phillips, A. D.; Olmstead, M. M.; Power, P. P. *J. Am. Chem. Soc.* **2003**, *125*, 3204. (c) Abraham, M. Y.; Wang, Y.; Xie, Y.; Wei, P.; Schaefer, H. F., III; Schleyer, P. v. R.; Robinson, G. H. *J. Am. Chem. Soc.* **2011**, *133*, 8874. (d) Waterman, R.; Hayes, P. G.; Tilley, T. D. *Acc. Chem. Res.* **2007**, *40*, 712. (e) Zhang, S.-H.; Yeong, H.-X.; Xi, H.-W.; Lim, K. H.; So, C.-W. *Chem.—Eur. J.* **2010**, *16*, 10250. (f) Jana, A.; Leusser, D.; Objartel, I.; Roesky, H. W.; Stalke, D. *Dalton Trans.* **2011**, *40*, 5458. (g) Rodriguez, R.; Gau, D.; Contie, Y.; Kato, T.; Saffron-Merceron, N.; Baceiredo, A. *Angew. Chem., Int. Ed.* **2011**, *50*, 11492. (h) Stoelzel, M.; Präsang, C.; Inoue, S.; Enthaler, S.; Driess, M. *Angew. Chem., Int. Ed.* **2012**, *51*, 399.

(6) For an introduction to ¹¹⁹Sn Mössbauer spectroscopy, see: (a) Spijkerman, J. J. In *The Mössbauer Effect and its Application in Chemistry*; Gould, R. F., Ed.; American Chemical Society: Washington, DC, 1967; Advances in Chemistry Series, Vol. 68, p 105. (b) Greenwood, N. N.; Gibb, T. C. *Mössbauer Spectroscopy*; Chapman & Hall: London, U.K., 1971; p 371. (c) Zuckerman, J. J. In *Chemical Mössbauer Spectroscopy*; Herber, R. H., Ed.; Plenum Press: New York, 1984; p 267.

(7) Al-Rafia, S. M. I.; McDonald, R.; Ferguson, M. J.; Rivard, E. *Chem.—Eur. J.* **2012**, *18*, 13810.

(8) Al-Rafia, S. M. I.; Malcolm, A. C.; Liew, S. K.; Ferguson, M. J.; McDonald, R.; Rivard, E. *Chem. Commun.* **2011**, *47*, 6987.

(9) Pangborn, A. B.; Giardello, M. A.; Grubbs, R. H.; Rosen, R. K.; Timmers, F. J. *Organometallics* **1996**, *15*, 1518.

(10) Jafarpour, L.; Stevens, E. D.; Nolan, S. P. *J. Organomet. Chem.* **2000**, *606*, 49.

(11) Balch, A. L.; Oram, D. E. *Organometallics* **1988**, *7*, 155.

(12) Mansell, S. M.; Herber, R. H.; Nowik, I.; Ross, D. H.; Russell, C. A.; Wass, D. F. *Inorg. Chem.* **2011**, *50*, 2252.

(13) Cohen, S.; Ma, J.; Butenschön, H.; Herber, R. H. *Dalton Trans.* **2009**, 6606.

(14) <http://www.megadaq.com>.

(15) Hope, H. *Prog. Inorg. Chem.* **1994**, *41*, 1.

(16) Blessing, R. H. *Acta Crystallogr.* **1995**, *A51*, 33.

(17) Sheldrick, G. M. *Acta Crystallogr.* **2008**, *A64*, 112.

(18) Altomare, A.; Burla, M. C.; Camalli, M.; Casciaro, G. L.; Giacovazzo, C.; Guagliardi, A.; Moliterni, A. G. G.; Polidori, G.; Spagna, R. *J. Appl. Cryst.* **1999**, *32*, 115.

(19) Beurskens, P. T.; Beurskens, G.; de Gelder, R.; Garcia-Granda, S.; Gould, R. O.; Smits, J. M. M. *The DIRDIF2008 Program System*; Crystallography Laboratory, University of Nijmegen: Nijmegen, The Netherlands, 2008.

(20) For prior work in this field, see: (a) Marks, T. J.; Newman, A. R. *J. Am. Chem. Soc.* **1973**, *95*, 769. (b) Petz, W. *Chem. Rev.* **1986**, *86*, 1019. (c) Holt, M. S.; Wilson, W. L.; Nelson, J. H. *Chem. Rev.* **1989**, *89*, 11. (d) Rugar, P. A.; Jennings, M. C.; Ragogna, P. J.; Baines, K. M. *Organometallics* **2007**, *26*, 4109. (e) Ghadwal, R. S.; Azhakar, R.; Pröpper, K.; Holstein, J. J.; Dittrich, B.; Roesky, H. W. *Inorg. Chem.* **2011**, *50*, 8502. (f) Iovkova-Berends, L.; Berends, T.; Zöller, T.; Schollmeyer, D.; Bradtmöller, G.; Jurkschat, K. *Eur. J. Inorg. Chem.* **2012**, *21*, 3463. For related studies, see: (g) Vogel, U.; Timoshkin, A. Y.; Scheer, M. *Angew. Chem., Int. Ed.* **2001**, *40*, 4409. (h) Mathey, F.; Huy, N. H. T.; Marinetti, A. *Helv. Chim. Acta* **2001**, *84*, 2938. (i) Aktas, H.; Slootweg, J. C.; Lammertsma, K. *Angew. Chem., Int. Ed.* **2010**, *49*, 2102.

(21) Because of nonresonant scattering of gamma ray absorption, which scales with Z , the magnitude of the Mössbauer effect in W compounds is significantly reduced relative to that observed in homologous Cr complexes.

(22) It should be mentioned that any correlation of $C_{IP}-E$ bond distances ($E =$ Group 14 element) with bond strengths should be done with caution given that in the case of theoretically analyzed germylene-carbene adducts ($NHC \cdot GeR_2$), bond length changes of up to 0.04 \AA (as R was varied) did not lead to direct correlations with the calculated carbene-germylene interaction energies. Ruddy, A. J.; Rugar, P. A.; Bladek, K. J.; Allan, C. J.; Avery, J. C.; Baines, K. M. *Organometallics* **2010**, *29*, 1362.

(23) (a) MacDonald, E.; Doyle, L.; Chitnis, S. S.; Werner-Zwanziger, U.; Burford, N.; Decken, A. *Chem. Commun.* **2012**, *48*, 7922. (b) MacDonald, E.; Doyle, L.; Burford, N.; Werner-Zwanziger, U.; Decken, A. *Angew. Chem., Int. Ed.* **2011**, *50*, 11474 and references therein.

(24) Maddock, A. G. *Mössbauer Spectroscopy: Principles and Applications*; Horwood: Chichester, U.K., 1997; Chemical Science Series, pp 79–100.

(25) Nowik, I.; Spinney, H. A.; Richeson, D. S.; Herber, R. H. *J. Organomet. Chem.* **2007**, *692*, 5680.

(26) (a) Herber, R. H.; Smelkinson, A. E. *Inorg. Chem.* **1978**, *17*, 1023. (b) Drew, M. G. B.; Nicholson, D. G. *J. Chem. Soc., Dalton Trans.* **1986**, 1543.

(27) Bent, H. A. *Chem. Rev.* **1961**, *61*, 275.

(28) Rivard, E.; Fischer, R. C.; Wolf, R.; Peng, Y.; Merrill, W. A.; Schley, N. D.; Zhu, Z.; Pu, L.; Fettingner, J. C.; Teat, S. J.; Nowik, I.; Herber, R. H.; Takagi, N.; Nagase, S.; Power, P. P. *J. Am. Chem. Soc.* **2007**, *129*, 16197.

(29) Power, P. P.; Stanciu, C.; Nowik, I.; Herber, R. H. *Inorg. Chem.* **2005**, *44*, 9461.

(30) (a) See the discussion in references 6b (pp 400–401) and 6c (p 279), and references therein. (b) Herber, R. H.; Parisi, G. I. *Inorg. Chem.* **1966**, *5*, 769.

(31) Grynkewich, G. W.; Ho, B. Y. K.; Marks, T. J.; Tomaja, D. L.; Zuckerman, J. J. *Inorg. Chem.* **1973**, *12*, 2522.

(32) Cornwell, A. B.; Harrison, P. G. *J. Chem. Soc., Dalton Trans.* **1975**, 1486.

(33) (a) Herber, R. H.; Nowik, I.; Mochida, T. *J. Organomet. Chem.* **2011**, *696*, 1698. (b) Butenschön, H.; Ma, J.; Daniliuc, C. G.; Nowik, I.; Herber, R. H. *Dalton Trans.* **2011**, 3671.